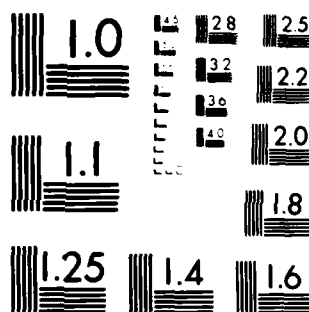END
DATE
FILMED

8-84

DTIC

MICROCOPY RESOLUTION TEST CHART
NATIONAL BUREAU OF STANDARDS 1963 A

A NUMERICAL SIMULATION STUDY OF SOLAR WIND DISTURBANCES RESPONSIBLE FOR GEOMAGNETIC AND AURORAL STORMS

S.-I. Akasofu

Geophysical Institute
University of Alaska
Fairbanks, Alaska   99701

AD-A144 178

Final Report
11 December 1980 - 11 November 1983

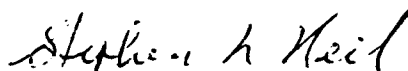31 January 1984

DTIC
ELECTE
AUG 9 1984

B

DTIC FILE COPY

84 08 09 059

This report has been reviewed by the ESD Public Affairs Office (PA) and is releasable to the National Technical Information Service (NTIS).

This technical report has been reviewed and is approved for publication.
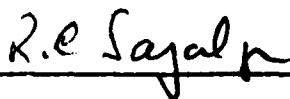
Richard C. Altrock
Contract Manager

S. L. Keil
Branch Chief

FOR THE COMMANDER

R. C. Sagalyn
Division Director

Qualified requestors may obtain additional copies from the Defense Technical Information Center. All others should apply to the National Technical Information Service.

If your address has changed, or if you wish to be removed from the mailing list, or if the addressee is no longer employed by your organization, please notify AFGL/DAA, Hanscom AFB, MA 01731. This will assist us in maintaining a current mailing list.

Do not return copies of this report unless contractual obligations or notices on a specific document require that it be returned.

REPORT DOCUMENTATION PAGE		READ INSTRUCTIONS BEFORE COMPLETING FORM
1. REPORT NUMBER AFGL-TR-84-0048	**2. GOVT ACCESSION NO.** AD-A144 178	**3. RECIPIENT'S CATALOG NUMBER**
4. TITLE *(and Subtitle)* A NUMERICAL SIMULATION STUDY OF SOLAR WIND DISTURBANCES RESPONSIBLE FOR GEOMAGNETIC AND AURORAL STORMS		**5. TYPE OF REPORT & PERIOD COVERED** Final Report 11 Dec 1980 – 11 Nov 1983
		6. PERFORMING ORG. REPORT NUMBER
7. AUTHOR(s) S.-I. Akasofu		**8. CONTRACT OR GRANT NUMBER(s)** F19628-81-K-0024
9. PERFORMING ORGANIZATION NAME AND ADDRESS Geophysical Institute University of Alaska Fairbanks, Alaska 99701		**10. PROGRAM ELEMENT, PROJECT, TASK AREA & WORK UNIT NUMBERS** 61102F 2311G3CA
11. CONTROLLING OFFICE NAME AND ADDRESS Air Force Geophysics Laboratory Sunspot, NM 88349 Monitor/Richard Altrock/PHS		**12. REPORT DATE** January 31, 1984
		13. NUMBER OF PAGES 34
14. MONITORING AGENCY NAME & ADDRESS*(if different from Controlling Office)*		**15. SECURITY CLASS. *(of this report)*** Unclassified
		15a. DECLASSIFICATION/DOWNGRADING SCHEDULE

16. DISTRIBUTION STATEMENT *(of this Report)*

Approved for public release; distribution unlimited

17. DISTRIBUTION STATEMENT *(of the abstract entered in Block 20, if different from Report)*

18. SUPPLEMENTARY NOTES

19. KEY WORDS *(Continue on reverse side if necessary and identify by block number)*

solar wind
solar flares
kinematic simulation
IMF magnitude

20. ABSTRACT *(Continue on reverse side if necessary and identify by block number)*

During the last 12 months, we have made significant progress in three areas, (i) the simulation of propagation of flare-generated shock waves, (ii) dynamo processes associated with solar flares; and (iii) the simulation of sunspot formation. During the next 12 months, we plan to extend our studies in the same three areas. Both some of the highlights and the future plans are fully described. Specifically, we have constructed a code to deal with the propagation of shock waves generated by six --->

DD $_{1\ JAN\ 73}^{FORM}$ **1473**   EDITION OF 1 NOV 65 IS OBSOLETE
S/N 0102-LF-014-6601

20. Abstract

successive flares and plan to study several observed events on the basis
of the code. We have developed a dynamo theory of the solar flares and
plan to simulate time-dependent models by an MHD simulation method.
We plan to examine observed velocity fields around sunspots in connection
with our dynamo theory of solar flares. It is also our plan to extend
our simulation study of sunspots by including magnetic buoyancy and
other factors.

Table of Contents

iii

I. Solar Wind Study by the Kinematic Simulation Method

During the last 12 months, we have developed a 3-D kinematic simulation method in order to be able to deal realistically with solar events. In particular, we have developed the computer code in order to be able to handle the propagation of shock waves generated by six successive solar flares from the same active region. We constructed first a steady state corotating pattern for the so-called 'two-sector' or 'two-stream' situation. For this purpose the distribution of the solar wind speed on the source surface (a spherical surface of radius of 2.5 $R_\odot$) is assumed to have the minimum speed ($V = 300$ km/sec) along the heliomagnetic equator, which is assumed to be inclined by $20°$ with respect to the heliographic equator; the speed is assumed to increase toward higher latitudes in both the northern and southern hemispheres. In this way, a fast and a slow solar wind flow stream out alternatively along a radial line fixed in space.

The first step of our method is to construct an initial distance (R) - time (t) relationship for particles streaming out along a (solar) radial line fixed in space. From two R-t curves at two successive instants t_1 and t_2 ($t_2 - t_1 = \Delta t$), we construct the velocity (V) - distance (R) relationship. Although our method is basically kinematic, faster particles are not allowed to take over slower particles. This restriction alters the initial R-t relationship. We modify the initial R-t relationship until the resulting V-R relationship resembles closely an empirically constructed V-R relationship on the basis of space probe observations or of theoretical results; for the R-t and V-R relationships, see Figures 1.4a, 1.4b and 1.5 in Hakamada and Akasofu (1982). The final R-t relationship thus obtained becomes the basis for

1

our study. The magnetic field is compressed in the shocks; the flux density and field intensity can be computed using flux conservation. The resulting magnetic field configuration in the equatorial plane is the familiar corotating structure which consists of two 'spiral arms' (the corotating interaction region).

Effects of solar flares are introduced into this steady corotating pattern by adding a high speed flow from a circular area, centered around a solar flare. In the circular area, the flow speed is assumed to have a Gaussian distribution of the 'half-width' σ; the flow speed V_F at the center is assumed to vary with time as $V_F = V_{Fmax} \cdot t \cdot e^{-(t/\tau)}$; thus, a flare is characterized by six parameters, the latitude (θ), longitude (ϕ) and the onset time (T_F) of a flare, the maximum flow V_{Fmax} (km/sec) at the center of the circular area of size parameterized by $\sigma(°)$, and the time variations of V_{Fmax} by τ(hr).

The first flare is assumed to occur at $T = 0$ and at $\theta = 0°$, $\phi = 0°$. This particular flare is parameterized by the maximum wind speed $V_{Fmax} = 800$ km/sec, $\tau = 12$ hrs and $\sigma = 60°$. The second flare is introduced 48 hours (2 days) after the first flare. It is assumed that the same active region is responsible for the second flare; at the time of the second flare, the active region rotated by $\phi = 28.3°$ from the time of the first flare. The second flare is assumed to be characterized by a faster flow $V_{Fmax} = 1000$ km/sec, the same growth-decay curve ($\tau = 12$ hrs) and a narrower extent ($\sigma = 10°$) than the first one, and so on.

Figure 1 shows the disturbance patterns in the ecliptic plane at distances < 5 au at $T = 4.0$, 5.0, 6.0 and 7.0 days after the onset of the first flare. At $T = 4.0$ days, the one can see that the familiar spiral structure of the interplanetary magnetic field with the two 'spiral

2

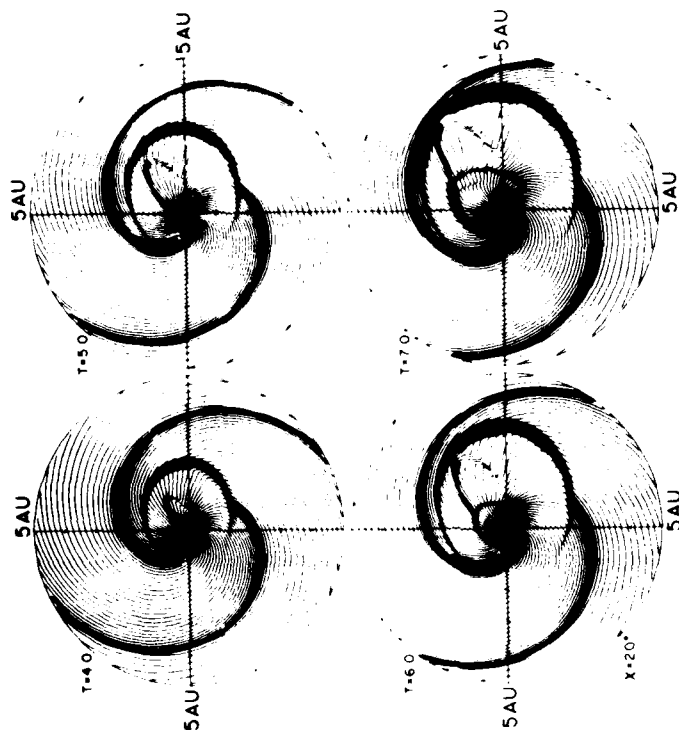Figure 1. Solar wind disturbances caused by successive flares in the ecliptic plane, from the same active region. The spiral curves indicate the magnetic field lines in the ecliptic plane. The figure shows the propagating structure at 4.0, 5.0, 6.0 and 7.0 days after the onset of the first flare. The shock waves cause narrow belts of concentrated magnetic fluxes. The outer limit of each circular area is at 5 au.

arms', but one of them is disturbed by the two shock waves. The third flare began at T = 4.0 days, but the associated shock wave is too close to the sun at that time.

At T = 5.0 days, the shock wave caused by the third flare becomes evident. The fourth flare occurred at that time. At T = 6.0 days, the shock wave associated with the fourth flare becomes evident. The second shock wave catches up with the first shock wave because the former is associated with a faster flow than the second flow.

At T = 7.0 days, the first and second shock waves reach one of the spiral arms at a distance of ~ 4 au. Note that the two spiral arms rotate steadily with the sun during the entire period. Note also that the fifth flare begins at that time. Figure 2 shows the disturbance pattern within a radial distance of < 15 au, at T = 7, 10, 15, 17, 19 and 25 days after the onset of the first flare. At T = 10 days, the last (sixth) flare took place.

One can easily see that the shock waves and the corotating spiral arms interact, forming a large-scale magnetic structure and expanding rapidly outward. The corotating structure in the inner heliosphere was destroyed by the successive shock waves. However, after the last flare which took place at T = 10 days, it begins to reform near the sun. It is clearly seen at T = 25 days; see the arrow in the figure.

McDonald et al. (1981) observed a large decrease of galactic cosmic ray intensity (in the outer heliosphere) a few months after successive flare activities in April 1978 and March, April and May 1979. As suggested by Burlaga (1982) and Intriligator and Miller (1982), it is quite likely that the flare-induced shocks and corotating structure have profound effects on the propagation of both galactic and solar cosmic ray
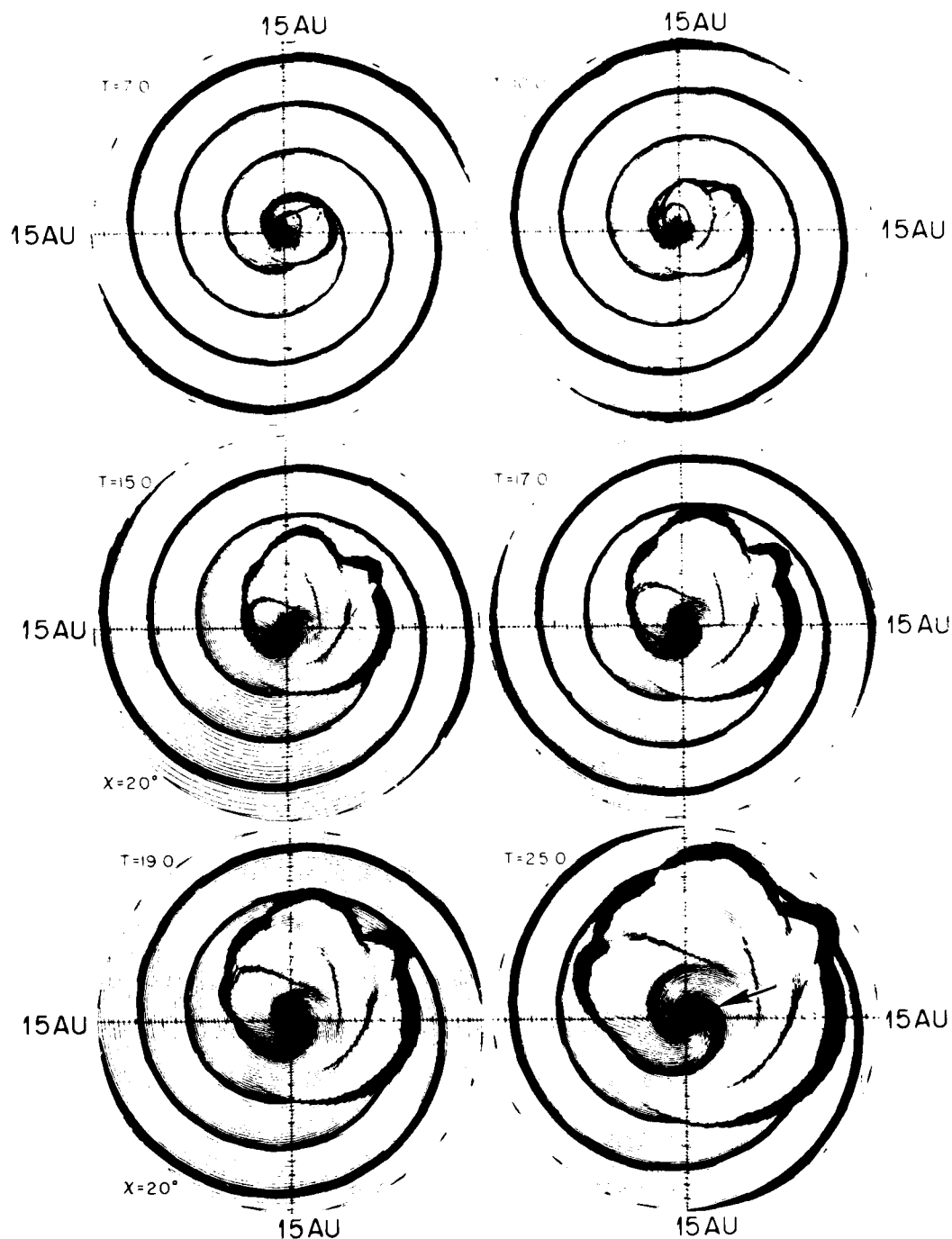
Figure 2. Solar wind disturbances caused by six successive flares during a period of 10 days. The figure shows the propagating structure at T = 7.0, 10.0, 17.0, 15.0, 19.0 and 25.0 days after the onset of the first flare. The outer limit of each circular area is at 15 au.

particles in the outer heliosphere by forming a sort of barrier to them.

It should be noted that the present study is a kinematic one in which a simple, empirical method (Hakamada and Akasofu, 1982) is used to provide a first order construction, temporally and spatially, of flare-generated shocks and their multiple interactions with each other as well as with corotating interaction regions. It is hoped that such a first order effort will be of some use in interpreting solar wind and cosmic ray observations by space probes. We have not simulated the other dynamic, thermodynamic, and magnetic properties (other than first-order IMF distortion) that can be found only from the MHD solutions such as those by Wu et al. (1979, 1983), Dryer et al. (1980) and D'Uston et al. (1981).

Figure 3 shows the computed V-t relationship for the situation described in the above. It may be compared with an observation of the solar wind by two space probes, Voyager 1 ($\sim$ 8 au) and Helios 1 ($\sim$ 0.5 au) in Figure 4. The velocity profiles at 1.0 and 10.0 au in Figure 3 are similar to those observed by the Helios and Voyager, respectively. These and other results will be published in the following two papers.

S.-I. Akasofu and K. Hakamada, Solar wind disturbances in the outer heliosphere, caused by six successive solar flares from the same active region, Geophys. Res. Lett., (in press), 1983.

S.-I. Akasofu, K. Hakamada, and C. Fry, Solar wind disturbances caused by solar flares: Equatorial plane, Planet. Space Sci., (in press), 1983.
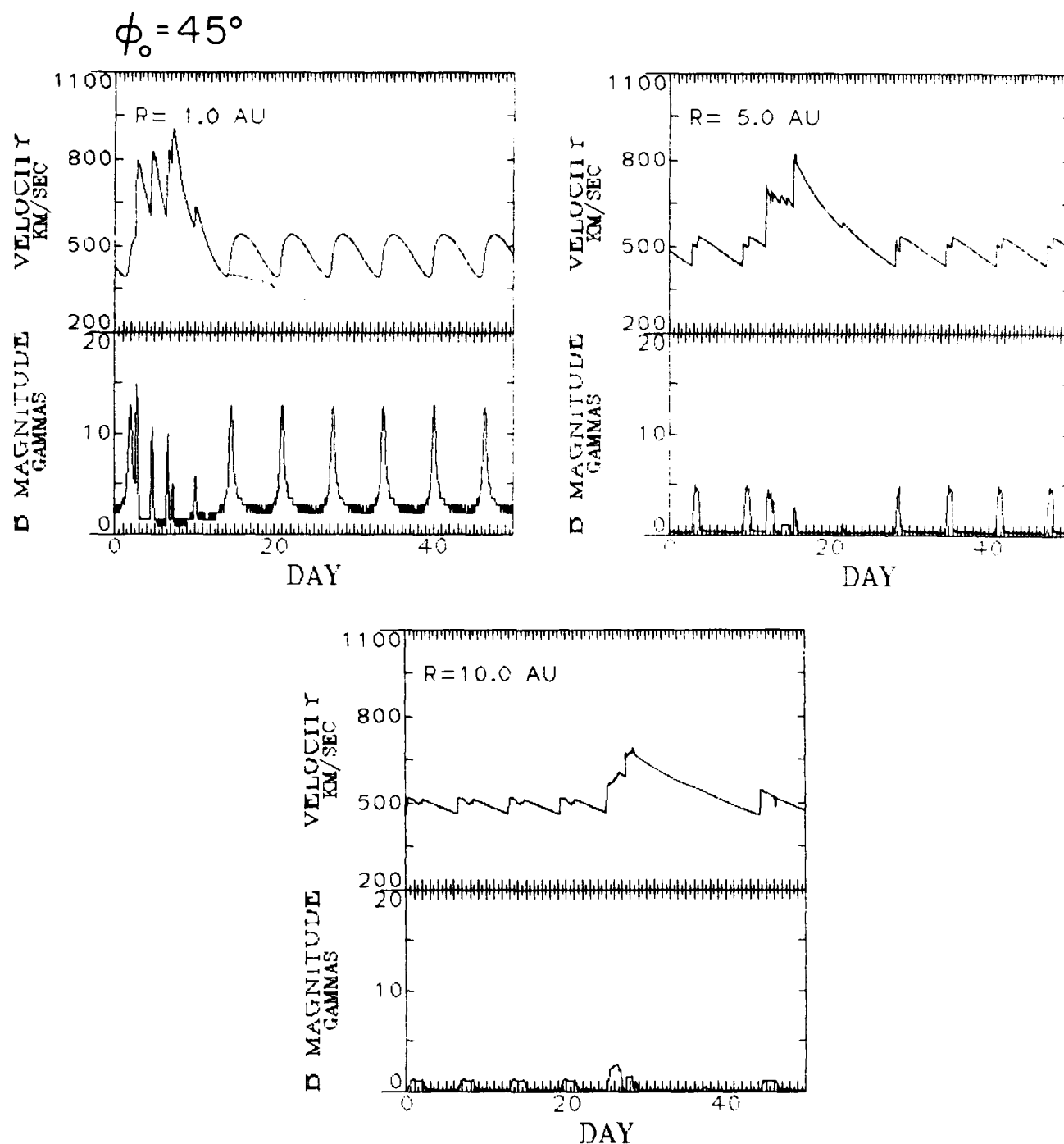
Figure 3. The time variations of the solar wind and the IMF magnitude at a radial distance of 1, 5 and 10 au along the radial line of longitude $\Phi_0 = 45°$; Φ_0 is reckoned counterclockwise from the righthand horizontal axis.

7
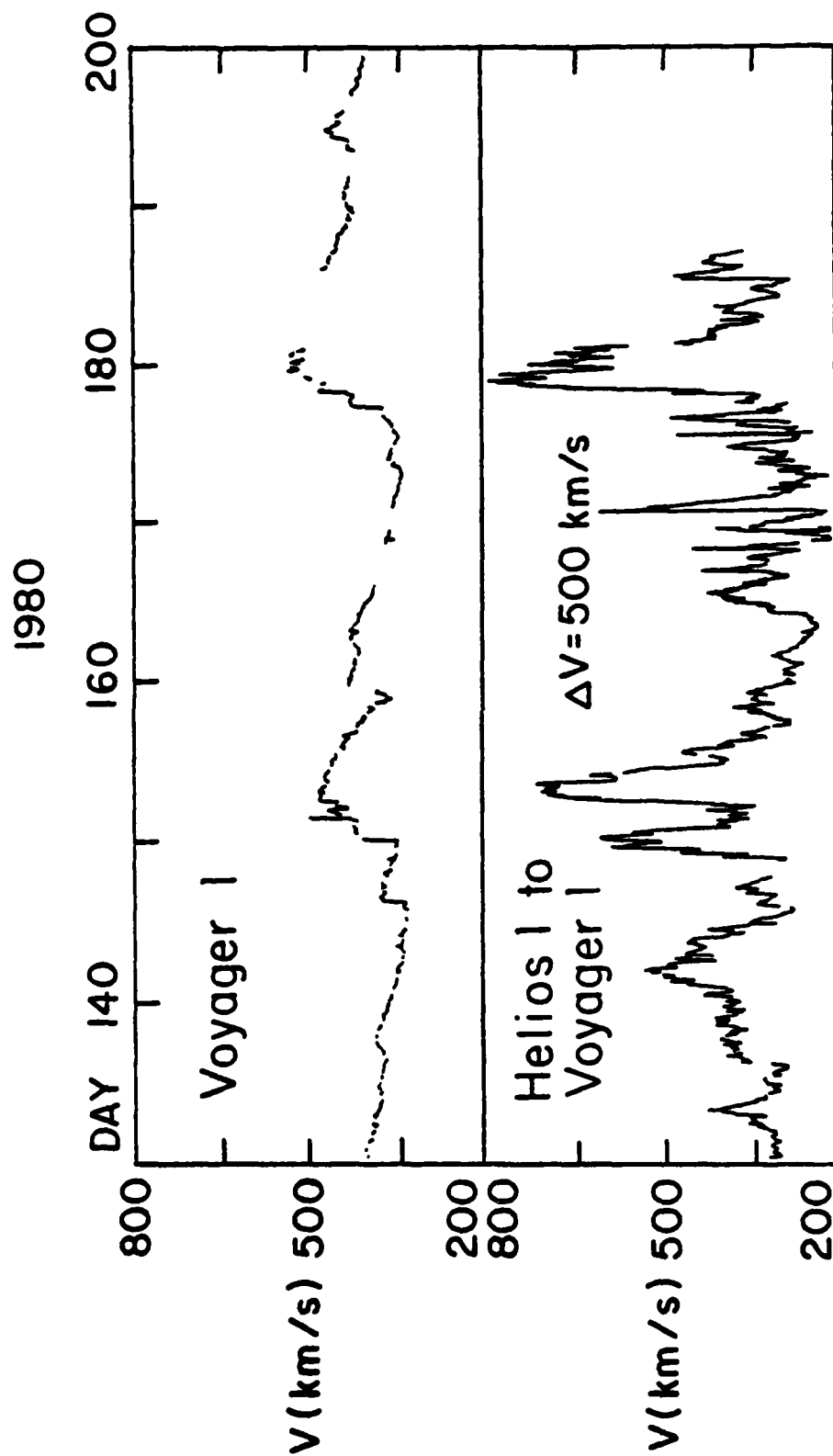
Figure 4. The solar wind speed observation by Voyager 1 at a radial distance of 7.5 ~ 8.5 au and by Helios 1 at a radial distance of ± 0.5 au (with a time delay assuming a constant speed of 500 km/sec); after Burlaga et al. (1983).

8

At present we are studying the following two events:

1. November 22 - December 6, 1977

    This was a unique period during which data from six spacecraft
    are available, and the observation was summarized in detail by
    Burlaga et al. (1979) in their paper entitled Interplanetary
    particles and fields, November 22 - December 6, 1977: Helios,
    Voyager, and Imp observations between 0.6 au and 1.6 au."

2. June - July 1, 1982

    There were three active regions which produced a large number
    of flares. There are deep space probe data (Pioneer 10 and 11)
    during this period.

II. Calibration of the Kinematic Method of Studying the Solar Wind on the
Basis of a One-dimensional MHD Solution

The empirical kinematic method (the HA method) can be improved by
having a theoretical or observational velocity (V) - distance (R)
relationship. Thus, it is important to make every effort to improve the
HA method on the basis of MHD solutions (the V-R relationship). Once the
improvement is made, the HA method becomes a powerful tool in inferring
the solar wind flow and the interplanetary magnetic field configuration
in the heliosphere. We shall show some of the new results which are
obtained using the new V-R relationship.

We assume that the interplanetary medium can be represented as a
single fluid with negligible dissipation. In terms of the spherical
coordinates (r, θ, ϕ) the dependent variables are density ρ, thermal
pressure p, fluid velocity $(V_r, 0, V_\phi)$. The independent variables are

radius r and time t. With these assumptions, and using MKS units the MHD equations to be solved, in the ecliptic plane, are as follows:

$$\frac{\partial}{\partial t}\left(r^2\rho\right) + \frac{\partial}{\partial r}\left(r^2\,\rho V_r\right) = 0 \tag{1a}$$

$$\frac{\partial}{\partial t}\left(r^2\rho V_r\right) + \frac{\partial}{\partial r}\left[r^2\,\rho V_r^{\;2} + p + \frac{B_\phi}{2\mu}\right] = 2rp + r\rho V_\phi^{\;2} - \rho GM_s \tag{1b}$$

$$\frac{\partial}{\partial t}\left(r^2\rho V_\phi\right) + \frac{\partial}{\partial r}\left[r^2\,\rho V_r V_\phi - \frac{B_r B_\phi}{\mu}\right] = r\,\frac{B_r B_\phi}{\mu} - \rho V_r V_\phi \tag{1c}$$

$$\frac{\partial}{\partial t}\left[r^2\left\{\frac{p}{\gamma-1} + 1/2\rho(V_r^{\;2} + V_\phi^{\;2}) + \frac{1}{2\mu}(B_r^{\;2} + B_\phi^{\;2})\right\}\right]$$

$$+ \frac{\partial}{\partial r}\left[r^2 V_r\left\{\frac{\gamma p}{\gamma-1} + 1/2\,\rho(V_r^{\;2} + V_\phi^{\;2})\right\}\right] \tag{1d}$$

$$\frac{\partial}{\partial t}\left(rB_\phi\right) + \frac{\partial}{\partial r}\left[r(V_r B_\phi - V_\phi - V_\phi B_r)\right] = 0 \tag{1e}$$

$$\frac{\partial}{\partial t}\left(rB_r\right) = 0 \tag{1f}$$

The various constants appearing in the above equations are: the rate of specific heat γ, the magnetic permeability μ, the gravitational constant G, and the solar mass M_s.

Because of a great difference of the two methods, however, it is not possible to have the same initial and boundary conditions for this comparison. In our MHD simulation a radial velocity

$$V_r = 300.0 + 313.4\,\sin^2(\Omega t) \tag{2}$$

is assumed and maintained at r = 0.5 au for all t>0, which provides a valid solution beyond the critical point. The constant Ω is chosen so that $2\pi/\Omega$ = 25.4 days, the solar rotation period. A discussion of the finite difference method of solving the MHD equations, as well as the initial state of the solar wind, may be found in Steinolfsen, et al. (1975). Computations are carried out to 10 AU by Dryer and Smith (private communication). We ran the computation until the first shock advanced well beyond a distance of 10 au. Figure 5 shows the V-R relationship at T = 2161.89 hours ($\sim$ 90 days).

The HA method requires the following parameters: A, B, τ_1, τ_2, V_o, $\alpha = (R(a) - R(b))/(R(a) - R(c))$; details are given in Hakamada and Akasofu (1982). Figure 5 includes the V-R relationship and the R-t relationship for the following set of parameters at T = 90 days = 2160 hr:

$$A = 0.15 \qquad\qquad V_o = 480 \text{ km/sec}$$

$$B = 0.85 \qquad\qquad \alpha = 0.7 \exp\left\{-2 \cdot 10^{-5} \left(|\Delta t| - 423\right)^2\right\}$$

$$\tau_1 = 30000 \text{ hr} \qquad\qquad \text{for } 0 < |\Delta t| < 423 \text{ hrs}$$

$$\tau_2 = 550 \text{ hr} \qquad\qquad \alpha = 0.7 \text{ for } 423 \text{ hr} < \Delta t$$

It is quite likely that a number of sets of the parameters can make a reasonable fit. However, the non-uniqueness is not the problem, since what matters is the V-R and R-t curve which can reproduce accurately the MHD solutions. In spite of the fact that an exact comparison is not possible (because of differences of the origin and of a minor difference of the time variations of solar wind speed at the source), the agreement between the two curves is reasonable.
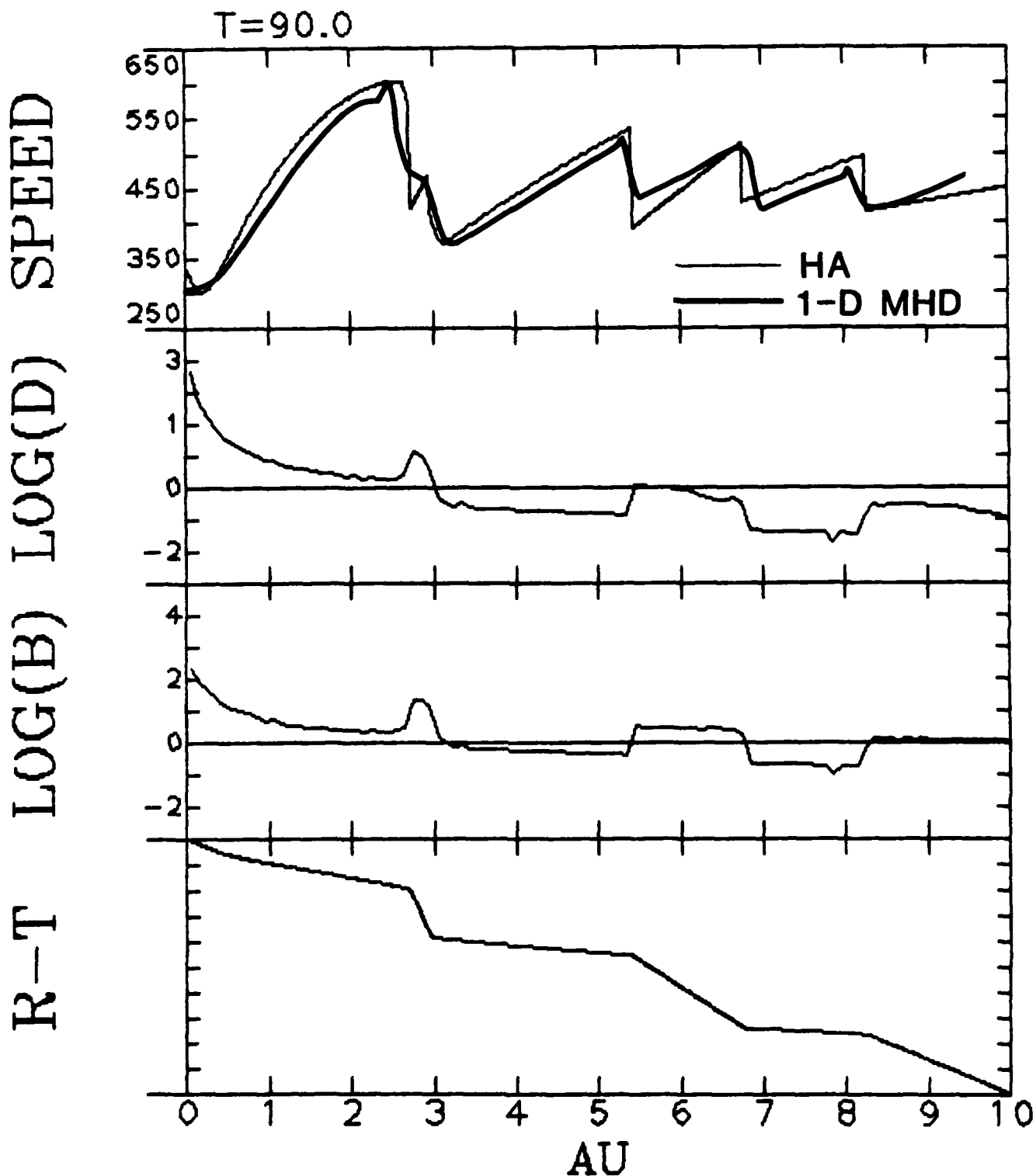
11

Figure 5. Comparison of the velocity V – distance R relationships obtained by the HA method and a one-D MHD simulation. It shows also the density and the magnetic field magnitude as a function of R obtained by the HA method; the results from the one-D solution are essentially identical to those obtained by the HA method.

An important point to make here is that it is relatively easy to modify the R-t curve in such a way that the resulting V-r curve resembles quantitatively a solution of the MHD equations. Taking into account various uncertainties involved in obtaining the MHD solutions, the agreement between the two V-R curves should be considered satisfactory at the present time. If improved one-dimensional solutions or two-, three-dimensional solutions become available, the modification could be similarly made. If space probe observations could eventually provide an accurate V-R relationship, our V-R curves would also be improved by the same procedure.

In concluding, it is interesting to consider why a crude kinematic method can reproduce reasonably well the MHD solution. This is because the solar wind flow is a relatively simple gas flow, compared with, say, motions of the terrestrial atmosphere. In spite of the fact that the collisionless solar wind plasma has a variety of complicated internal processes, there is no major internal heat source and boundaries which alter radically the initial flow speed, except in the vicinity of the planets which have, however, trivial obstacles in the heliospheric scale. As a result, the R-t relationship is well confined between the two curves which connect the maxima and minima in the original R-t curve. That is to say, the solar wind flow has a significant kinematic tendency. This tendency has recently been well illustrated by Burlaga et al. (1983) who showed that the solar wind speed observed at Voyager 1 ($\sim$ 8 au) can reasonably be inferred from Helios ($\sim$ 0.5 au) observation, except at the time of the passage of the shock waves. At the present time, we have been finding even a better method to improve the agreement.

III. A Dynamo Theory of Solar Flares

Most of the modern flare theories have been developed on the basis that the magnetic energy stored in the solar atmosphere is suddenly released by magnetic field reconnection or by current interruption. However, there has been little discussion of how the stored magnetic energy is generated. Regardless of any specific models of solar flares, it is important to treat the flare phenomenon in the context of an energy generation-dissipation system as a whole. On the basis of this thought, we have proposed a dynamo theory of solar flares. The reason for emphasizing the dynamo process is two-fold. The first is to propose that temporal variations of energy dissipated during a flare follow closely those of the dynamo power which can supply the required power of 10^{29} erg s^{-1} and total energy of 10^{32} erg. This is in contrast to the prevailing view that the energy for solar flares should be stored in the coronal magnetic field prior to flare onset. The second is to formulate the electrodynamic coupling of the photosphere-chromosphere-corona system, powered by the dynamo process, in which solar flares are a consequence of enhanced dynamo power output. Thus, we emphasize both energy generation and energy dissipation associated with solar flares.

The idea of powering solar flares by the dynamo process in the partially ionized chromosphere-photosphere region has been discussed earlier by several workers, including Sen and White (1972), Heyvaerts (1974), Obayashi (1975), Akasofu (1979). Certain aspects of these models are briefly reviewed here. Sen and White (1972) suggested that the dynamo-induced Hall current leads to Joule heating in the photosphere and that the electric field is anti-parallel to the convection velocity in the photospheric dynamo region. They suggested that a two-stream

14

instability (Farley, 1963) can occur in the Hall current to trigger a flare in the photosphere. Hayvaerts (1974) presented a photospheric dynamo model in which the coronal currents are entirely field-aligned and are driven by horizontal photospheric motions. Following Alfvén and Carlqvist (1967), Heyvaerts (1974) assumed that the coronal field-aligned currents can be interrupted by an instability (unspecified) and thereby release the stored magnetic energy to produce flares. Obayashi (1975) proposed a flare model similar to Hayvaerts (1974) except the suggestion that the release of the stored coronal energy is initiated by a collapse in the magnetic field and the formation of an X-type reconnection line in the corona. Recently, Akasofu (1979) emphasized that the dynamo process in the photosphere can supply the required power (10^{29} erg s^{-1}) and the total energy (10^{32} erg) and suggested that disruption of coronal field-aligned currents driven by the photospheric dynamo can lead to an electric potential structure which accelerates the current-carrying electrons to produce flares.

The proposed solar flare process to be developed in the present paper has evolved from the above-mentioned dynamo flare models (Sen and White, 1972; Heyvaerts, 1974; Obayashi, 1975; Akasofu, 1979). The important differences between the proposed model and those earlier models lie in (i) solar flares are treated self-consistently and quantitatively as a consequence of the electrodynamic coupling of the photosphere-chromosphere-corona system and (ii) the onset of flares is quantitatively identified as a result of the development of field-aligned potential drops due to the loss-cone constriction effect (Knight, 1973) on enhanced upward field-aligned currents, independent of any instabilities.

Consider now the photosphere-chromosphere-corona coupling system which is magnetically connected by arch-like (two-dimensional) field lines anchored in the photosphere, as schematically illustrated in Figure 6. A horizontal motion of the neutral gas in the photosphere and the lower chromosphere across the feet of the arch-like field lines constitutes a dynamo process. For simplicity, the dynamo region is assumed to consist of a shear flow of horizontal neutral wind V_n as indicated in Figure 6. The corona is located in the upper part of the arch and is primarily a reactive load (capacitive and inductive). The conjugate chromosphere-photosphere region is primarily a resistive load (hereafter referred to as the conjugate region).

As the suggested horizontal wind blows in the photosphere and the lower chromosphere (hereafter referred to as the dynamo region), dynamo currents are generated and flow through the whole system (the photosphere-chromosphere-corona), both along and across magnetic field lines. The power generated by the dynamo consists of power dissipated in the dynamo region and power output to the load. The output power delivered to the load is partially dissipated in the conjugate region; the remaining power is in part consumed to accelerate current-carrying particles along magnetic field lines and in part stored in the corona.

Suppose that the velocity of the wind in the dynamo region increases from a very low value. As the dynamo power increases, the intensity of the field-aligned currents will be enhanced. However, the upward field-aligned current density is limited by the 'loss-cone' effect on the precipitating coronal electrons, due to the converging magnetic field which exerts upward mirror forces on the precipitating electrons. The 'loss-cone' is defined by a downward facing solid-angle centered along

16
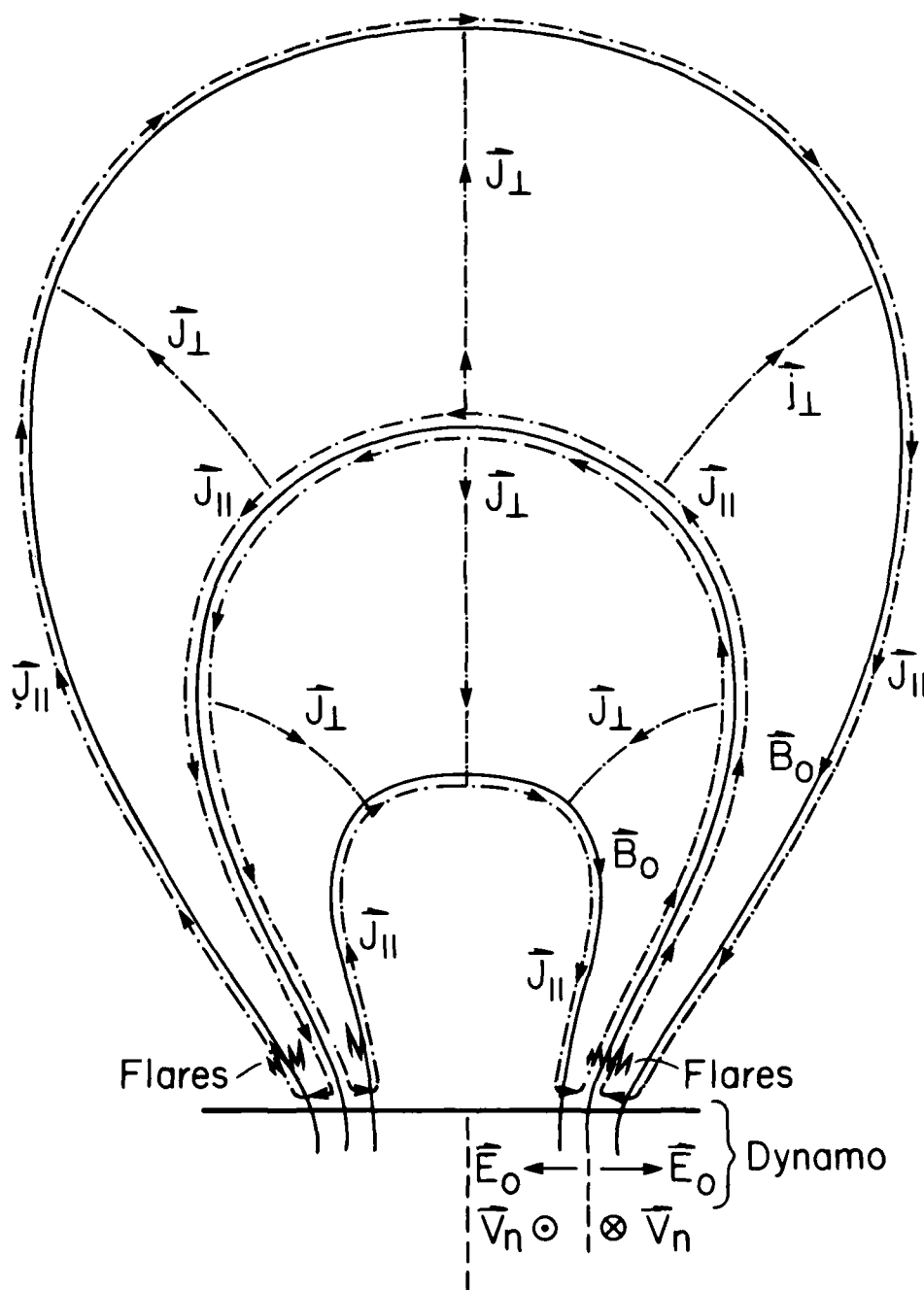
Figure 6. A schematic illustration of the photosphere-chromosphere-corona coupling system. The magnetic field B_0 has an arch-like configuration as indicated by solid curves. The dynamo region is located around the boundary between the photosphere and the lower chromosphere. Field-aligned current $J_{\parallel}$ and the cross-field current $J_{\perp}$ are illustrated by dash-dot curves. V_n is the neutral wind velocity. E_0 is the dynamo electric field.

the magnetic field. A particle whose pitch angle lies inside the loss-cone will reach the chromosphere-photosphere level. Once they reach this level, they will not be able to mirror back up the field lines due to charge-neutral collisions. Only those electrons inside the loss-cone can carry the upward field-aligned current to and from the dynamo region. Thus, the loss-cone effect imposes a limit on the upward field-aligned current density (Knight, 1973; Fridman and Lemaire, 1980). To exceed the loss-cone current limit, field-aligned potential drops are required to accelerate electrons and thereby reduce their pitch angles into the loss-cone. The required field-aligned potential drops can be distributed along field lines and supported self-consistently by the double layer process (for reviews see Fälthammar, 1978; Kan and Lee, 1981).

As the accelerated (upward current-carrying) electrons descend down along the legs of the arch toward the dynamo region and its conjugate region, they collide with the gases there, ionizing and exciting them. The resulting optical emissions are identified with the optical manifestation of flares during the rise phase excluding the impulsive phase (Kahler et al., 1980).

The most important aspect of our proposed mechanism is that the development of a flare follows closely the temporal variation of the power output from the dynamo process. Flare onset corresponds to the moment when the upward field-aligned current density exceeds the loss-cone limit and a significant potential drop is forced into existence along the magnetic field lines, accelerating the current-carrying electrons toward the lower chromosphere. The maximum epoch of a flare corresponds roughly the time when the dynamo power output maximizes. Our theory has been published:

18

Kan, J. R., S.-I. Akasofu, and L. C. Lee, A dynamo theory of solar

flares, Solar Phys., 84, 153, 1983.

In our theory, the velocity shear is crucial for flare production, and it is important to verify our theory on the basis of observations of velocity shear. It has been very fortunate that Harvey and Harvey (1980) have already examined the relationship between locations of the velocity shear in the photosphere and of solar flares. Figure 7 shows an example of their observation of a solar flare on April 28, 1978.

IV. A Simulation Study of the Formation of a Bi-polar Magnetic Structure

Emergence of magnetic flux through the photosphere and below has been discussed extensively in terms of magnetic buoyancy (Parker, 1955, 1979; Tandberg-Hanssen, 1967; Gilman, 1970; Schüssler, 1977, 1979; Moffatt, 1978; Meyer et al., 1979; Spruit, 1981). The dynamics of magnetic flux has mostly been discussed in terms of the pressure balance equation $p_{ex} = p_{in} + B^2/8\pi$, where p_{ex} and p_{in} denote the plasma pressure external and internal to a flux tube, respectively. However, such an equation may be applicable only for a situation in which the flux tube rises as a whole along an extensive horizontal length (much longer than the extent of its vertical motion). It will be hardly applicable for a situation envisaged by Babcock (1961), in which the flux tube rises locally with a Ω-shaped geometry by a convective motion, such a distortion of a flux tube encounters a strong Lorentz force which tends to restore the initial straight geometry.

Recently, Gaizauskas et al. (1982) and Wallenhorst and Topka (1982) showed that a "complex of activity" is maintained by fresh injections of flux which forms and disappears in rapid succession as closely-spaced but

Figure 7.   Boulder region 1092 on April 28, 1978.   Each frame covers an area
of 256 by 256 arc seconds with north to the left and east to the top.   (top
left) Velocity image with black representing approach and white recession.
(top right) Velocity shear image with x's indicating flare sites.   (bottom
left) Magnetic field with white representing a field toward the observer and
black away from the observer.   (bottom right) Intensity image.

distinct bi-polar units; most of the magnetic flux disappears in less than one rotation and principally in situ, without evidence of significant spreading. If magnetic buoyancy is the cause for the formation of a Ω-shaped geometry of the magnetic flux tube, and if it is powerful enough to overcome the counteracting Lorentz force, there would not be any other force to submerge it. Therefore, it is difficult to explain why the magnetic flux can disappear without spreading.

Therefore, we suggest that a convective motion is more important than magnetic buoyancy as the direct cause of the Ω-shaped magnetic flux tube thus arisen is submerged by the counteracting Lorentz force as the convective motion decays. The importance of the convective motion was discussed earlier by Weiss (1966). More recently, Schüssler (1979) considered vertical motions generated by magnetic buoyancy. Meyer et al. (1979) examined buoyant magnetic flux tubes in supergranules. Parker (1982) examined effects of flux tubes on convection. The importance of the convective motion on this subject was also recently emphasized by Raadu (1983).

On the basis of the above consideration, we examined the formation and disappearance of a bi-polar magnetic structure from a horizontal magnetic field structure by a two-dimensional MHD simulation method by assuming initially well-defined convective cells which are allowed to evolve as they interact with the magnetic field.

The interaction between the photospheric gas and magnetic flux may be described by the standard MHD equations:

$$\frac{\partial \vec{B}}{\partial t} = \vec{\nabla} \times (\vec{v} \times \vec{B}) + \lambda \nabla^2 \vec{B} \tag{1}$$

$$\frac{d\vec{v}}{dt} = -\frac{1}{\rho} \vec{\nabla}p + \frac{1}{4\pi\rho} (\vec{\nabla} \times \vec{B}) \times \vec{B} + \vec{g} \qquad (2)$$

For the reasons given in the above, magnetic buoyancy is ignored as a first approximation by assuming that the mass density ρ is constant.

We choose for our model a characteristic length $L = 50,000$ km, and a characteristic velocity $V_o = 0.1$ km/sec in the first simulation and $V_o = 1$ km/sec in the second case. Such a choice of the values of L and V_o, together with the magnetic diffusivity $\lambda = 10^{-1}$ km^2/sec^{-1}, is equivalent to choose the magnetic Reynolds numbers of the order of $\lambda \times 10^3 \sim \times 10^4$, which are consistent with those used in the earlier studies (Weiss, 1966; Moffatt, 1978).

The MHD equations are solved by an explicit, two-dimensional, formulation of the Dufort-Frankel method. The one-dimensional Dufort-Frankel method is given in Potter (1973) and in Richtmeyer and Morton (1967). The method is appropriate for parabolic differential equations and is numerically stable for all time steps.

First of all, it is interesting to note that if we maintain the velocity pattern within the convective cell, we recover the earlier results obtained by Weiss (1966). Our result is shown in Figure 8 which may be compared with his Figure 4.

Let us assume that the initial velocity pattern is allowed to change. Figure 9 displays the magnetic and velocity field configurations at several stages. The time step for this experiment is $\Delta t = 3536$ sec $\approx$ 1 hr. The maximum fluid velocity is observed to decrease steadily with increasing time and the magnetic field lines are distorted into inverted "U" contours. Maximum distortion occurs within approximately at $32\Delta t$ or 1.3 days. The most important aspect of this particular simulation is
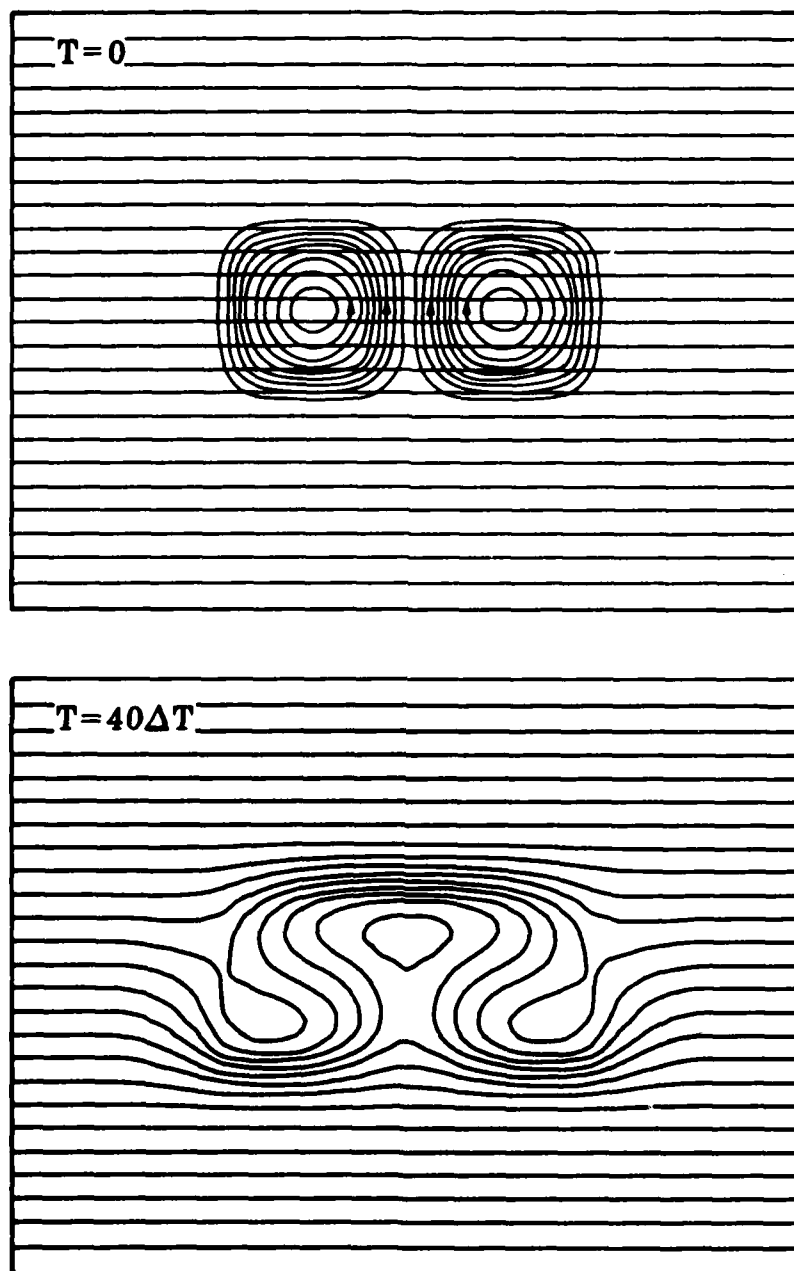
22

Figure 8. The deformation of a uniform magnetic field caused by a steady convective motion at T = 0 and about T = 40 hours after the onset of the convection.

23

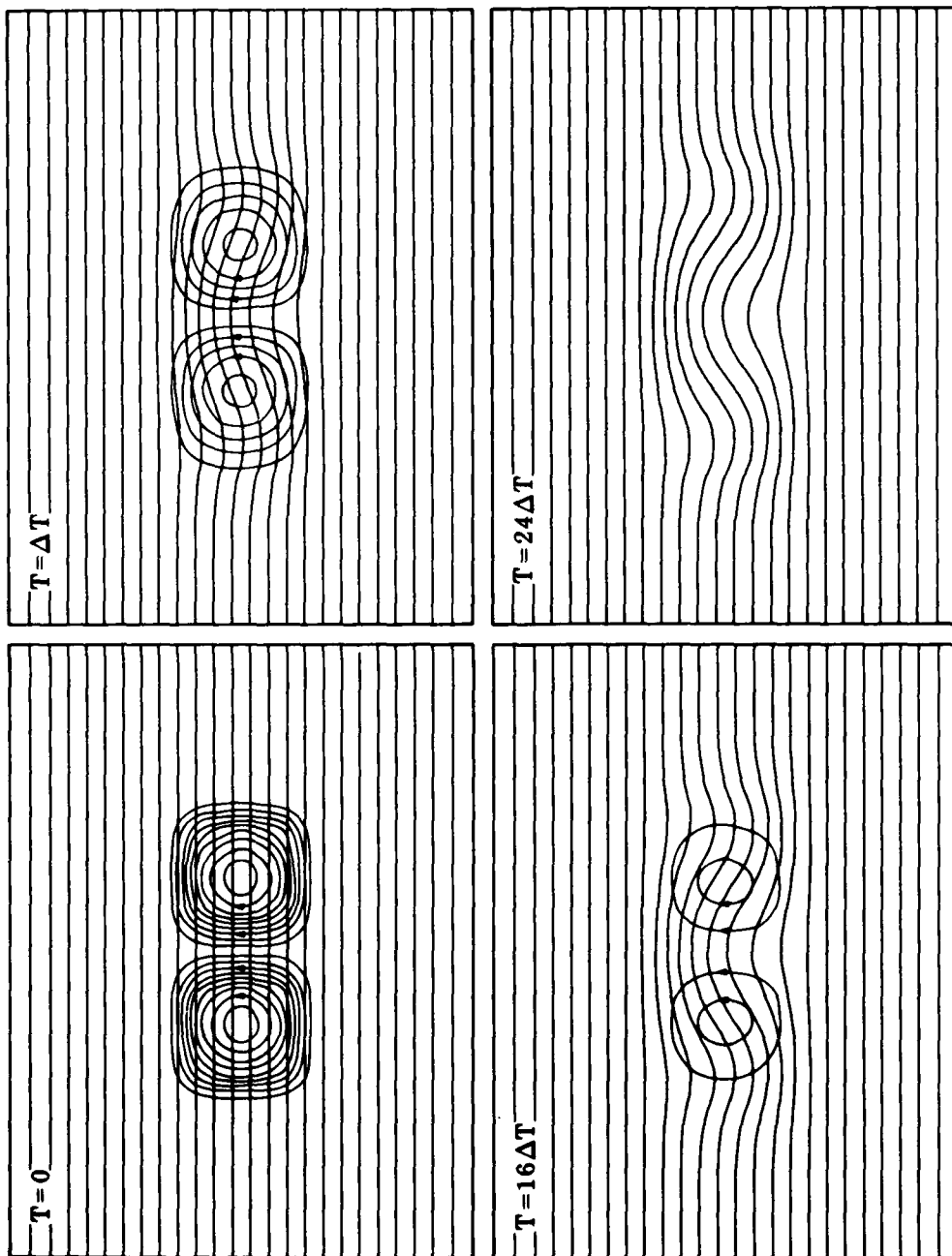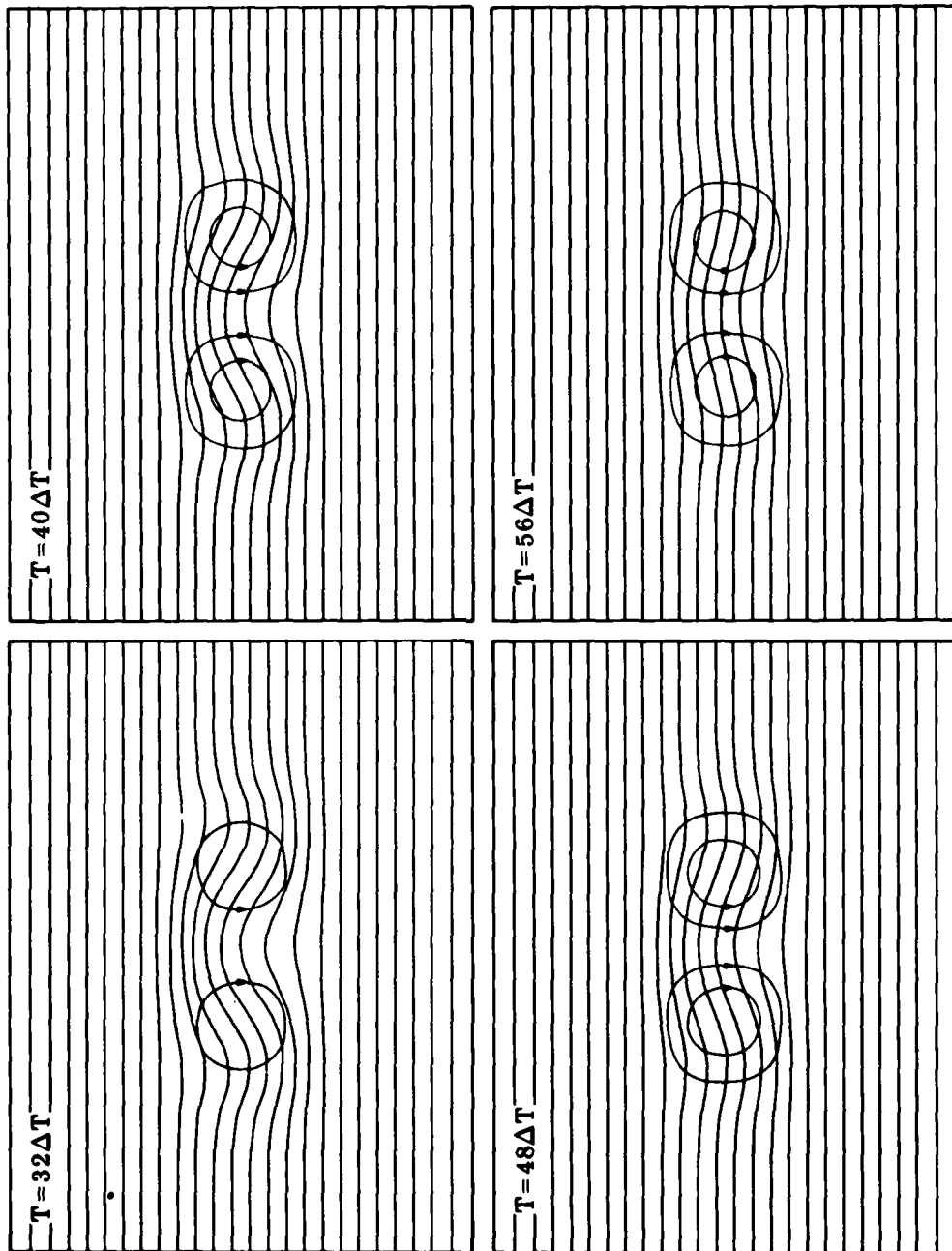Figure 9 (1)(2). The deformation of a uniform magnetic field caused by a convective motion at different epochs. The time step Δt is about 1 hr. In this case, the convective motion is given at $T = 0$ and let it interact with the magnetic field. It can be seen that the convective motion is reversed after about 1.3 days by the restoring Lorentz force.

24

T = 40ΔT

T = 56ΔT

T = 32ΔT

T = 48ΔT

25

that the convective motion has completely been reversed by the distorted magnetic field after the maximum distortion. At time t = 56Δt or about 2.3 days, the magnetic field has nearly returned to approximately its original position. As this process of "winding" and "unwinding" the field lines continue, the maximum absolute velocity tends to decrease.

Comparing Figure 8 and 9, it is interesting to speculate that the actual situation around sunspots is between them. The magnetic flux can maintain the Ω-shaped geometry, the counteracting Lorentz force tends to restore the initial horizontal configuration, forcing the Ω-shaped flux to submerge below the photosphere. This tendency may explain the new observations by Gaizauskas et al. (1982) and Wallenhorst and Topka (1982) that most of the magnetic flux in a complex of activity disappears rapidly in situ without evidence of significant spreading. Our results are reported in:

> Akasofu, S.-I. and G. Gislason, A simulation study of the formation of a bi-polar magnetic structure, Planet. Space Sci. (in press), 1984.

It is our plan to extend our simulation study of sunspot formation by including magnetic buoyancy and other factors.

V. A Study of the Relationship Between Sunspot Fields and Transient IMF Variations

The configuration of the magnetic field in the disturbed solar wind has long been an important topic for solar, cosmic ray and magnetospheric physicists (cf. Gold, 1962). This topic has particularly become very important in magnetospheric physics, since it has been found that the direction of the interplanetary magnetic field (IMF) is an important

factor in causing geomagnetic disturbances. Although both the solar wind speed V and the magnitude B of the IMF are also important and are expected to be large in the disturbed solar wind, the north-south component of the IMF (B_z) (accurately speaking, in the solar-magnetospheric coordinate system) plays a crucial role in determining the amount of solar wind energy to be transferred to the magnetosphere (cf. Arnoldy, 1971; Russell and McPherron, 1973; and Akasofu, 1981 and the references therein). Specifically, the amount of the transferred energy becomes very large when the IMF has a southward component ($\sim$ -20 nT for at least $\sim$ 6 hrs), causing intense magnetospheric and geomagnetic disturbances. On the other hand, when the IMF has a large northward component ($\sim$ +10 nT for several hours), the amount of the transferred energy becomes very small, resulting in only a weak disturbance.

The present large-scale IMF models do not provide such large values of the B_z component in the vicinity of the solar ecliptic plane (Parker, 1958). Thus, as in the past, most workers assume, implicitly or explicitly, that the B_z component is associated with the so-called 'magnetic tongue' (Gold, 1962), 'magnetic clouds' (Klein and Burlaga, 1982) and the wavy solar current disk (Smith, 1981; Akasofu 1981).

The magnetic tongue model has partially been supported by Pudovkin et al., (1976, 1977, 1979) who claimed that the degree of magnetic disturbances can be predicted by the north-south component of the photospheric magnetic field at the site of a solar flare, implying that the polarity of the IMF can be predicted from the flare field. Specifically, they showed that if a solar flare occurs in the region where the photospheric field has a southward component, the resulting geomagnetic disturbance tends to be intense, vice-versa. Their study

implies thus that the disturbed solar wind generated by a flare carries out the magnetic field from the flare region, retaining the same polarity of the field at least to a distance of 1 au. In a somewhat different context, Lundstedt et al. (1981) demonstrated that the solar wind speed tends to be high when the flare field has a southward component, while no high speed wind occurs when the flare field has a northward component. In addition, a bi-directional streaming of solar cosmic rays has also been considered as a supporting evidence of the magnetic tongue model (Palmer et al., 1978). As noted by Lundstedt (1982), however, one of the difficulties in this study is how to determine accurately the orientation of the magnetic field in the vicinity of solar flares. This is because the line of the polarity reversal (or the so-called 'neutral line') tends to run in the north-south direction, since sunspots in a pair tends to align in the east-west direction. Further, solar flares take place most often in a complex sunspot group. As a result, flare 'ribbons' have, in general, a very complicated geometry, curving in various directions. Therefore, it is a difficult task to determine a single value for the orientation (say, reckoned clockwise from the northward direction). The orientation of the magnetic field, which is most often directed across the flare ribbons, depends thus on where it is measured.

Tanaka (1979) found that there is a high degree of the occurrence of intense solar flares in the configuration called "delta spots" which are often formed by non-paired spots. In delta spots, the pair thus formed can often be oriented in the north-south direction or in the east-west direction (but opposite to Hale's law).

North-south oriented delta spots are of great interest here, since the line of the polarity reversal tends to align in the east-west

28

direction and thus the direction of the magnetic field in the vicinity of
solar flares can be inferred with reasonable accuracy. Tang (1982, 1983)
has already made an extensive study of delta spots and made their list
(1969-1979); here, the list is supplemented by including recent data
(1980-1982). Further, in this particular study, Tange et al. (1984, in
preparation) examine the IMF B_z component, instead of geomagnetic indices
which can be influenced by the solar wind speed V and the IMF magnitude
B, as well as by the B_z component.

VI. Results

Delta Configuration and Corresponding IMF

The McMath-Hulbert region 298 developed into a typical delta
configuration and passed the central meridian on September 22, 1979
(Tang, 1982; see Table 1). Figure 10 shows the Kitt Peak magnetogram,
the Boulder Hα filtagram, the Stanford magnetogram on September 22, 1979
(Solar-Geophysical Data, November 1979 (No. 423)). In the Kitt Peak
magnetogram, white portions on the disk indicate that the magnetic field
has a component toward the earth (positive), while dark portions have a
component away from the earth (negative). In the Stanford magnetogram,
solid and dashed lines indicate the positive and negative fields,
respectively. A large number of subflares and flares were observed in
the region between September 16 and 24 (some before and after this
period). As can be seen in the Kitt Peak and Stanford magnetograms, it
was the only prominent active region around the central meridian. The
positive polarity region was located directly north of the negative
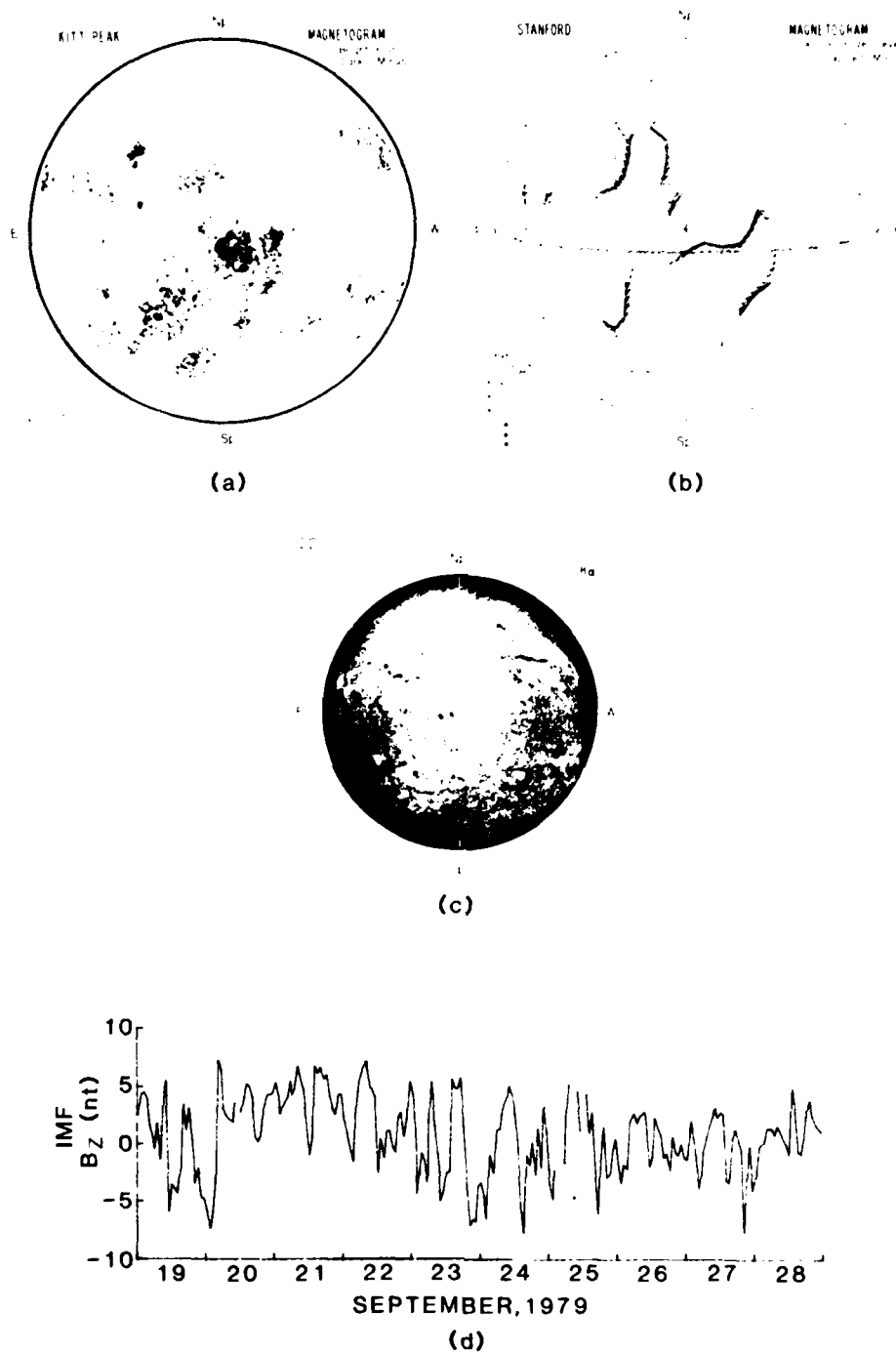polarity region. Such a polarity is described as N/S polarity for

29

SEPTEMBER 22, 1979

(a)

(b)

(c)

(d)

Figure 10. The Kitt Peak magnetogram, the Stanford magnetogram, the Boulder H_α filtergram on September 22, 1979 (Solar Geophysical Data) and the IMF B_z component between September 19 and 29, 1979 (ISEE-3).

30

convenience in describing the IMF orientation. The opposite polarity is described in the S/N polarity. The region produced one 3B flare on September 19, five 2B flares (September 16, 17, 18, 19) and a large number of IF, B flares as well. A medium magnetic disturbance began on September 19 and lasted until September 22. Another medium disturbance began on September 24 and lasted until November 1.

Figure 10 shows the IMF B_z component between September 19 and 29. It is clear that there was no obvious indication that the N/S polarity in the delta configuration extended to the earth's distance during or a few days after its passage across the central meridian.

We have just begun this study and must examine a large number of cases before any conclusion could be drawn. If we could find a simple relationship between the solar magnetic field orientation and the IMF B_z component, the degree of accuracy of predicting the occurrence and intensity of geomagnetic storms will increase considerably. Our preliminary results are, however, not necessarily very promising.

References

Akasofu, S.-I., Space Sci. Rev., 28, 121, 1981.

Akasofu, S.-I., Planet. Space Sci., 27, 1055, 1979.

Akasofu, S.-I., Solar Phys., 64, 333, 1979.

Alfvén, H., and P. Carlqvist, Solar Phys., 1, 220, 1967.

Arnoldy, R.L., J. Geophys. Res., 76, 5189, 1971.

Babcock, H. W., Ap. J., 133, 572, 1961.

Burlaga, L. F., EOS, 63, 1087, 1982.

Dryer, M., and Z. Smith, private communication, 1983.

Dryer, M., and E. Tandberg-Hanssen (ed), IAO Symposium No. 91, ᴿ. Reidel Pub.
    Co., 1980.

D'Uston, C., M. Dryer, S. M. Hans, and S. T. Wu, J. Geophys. Res., 86, 525,
    1981.

Fridman, M., and J. Lemaire, J. Geophys. Res., 85, 664, 1980.

Gaijanskas, V., Adv. Space Res., 2, 11, 1983.

Gaizauskas, V., Harvey, K. L., Harvey, J. W. and C. Zwaan, Ap. J., (in press)
    1982.

Gilman, P., Astrophys. J., 162, 1019, 1970.

Gold, T., Space Sci. Rev, 1962.

Hakamada, K., and S.-I. Akasofu, Space Sci. Rev., 31, 3, 1982.

Harvey, J.W., 21 May 1980, Adv. Space Res., 2, 31, 1983.

Harvey K., and J. Harvey, in Solar-Terrestrial Predictions Proceedings C-41,
    R. F. Donnelly (ed.), NOAA, 1980.

Hayvaerts, J., Solar Phys., 38, 419, 1974.

Intriligator, D. S., and W. D. Miller, J. Geophys. Res., 87, 4354, 1982.

Kahler, S., P. Spicer, Y. Uchida, and H. Zirin, in P. A. Sturrock (ed) Solar
    Flares, Colorado Assoc. Press, p. 85, 1980.

Kan, J. R., and L.-C. Lee, in S.-I. Akasofu and J. R. Kan (eds), Physics of Auroral Arc Formation, Geophys. Mono., AGU, 206, 1981.

King, J.H., Interplanetary Medium Data Book, NSSDC, NASA, Greenbelt, Maryland, 1977.

Klein, L.W., and C.F. Burlaga, J. Geophys. Res., 87, 613, 1982.

Knight, S., Planet. Space Sci., 21, 741, 1973.

Lundstedt, H., Solar Phys., 81, 293, 1982.

Lundstedt, H., J.M. Wilcox, and P.H. Scherrer, Science, 212, 1501, 1981.

Martin, S.F., L. Dezso, A. Antalova, A. Kucera, and K.L. Harvey, Adv. Space Res., 2 39, 1983.

McDonald, F. B., N. Lai, J. H. Trainor, M. H. I. Van Hollebeke, and W. R. Webber, Ap. J., 249, L71, 1981.

Moffatt, H. K. Magnetic Field Generated in Electrically Conducting Fluids, Cambridge Univ. Press, Cambridge, 1978.

Obasyashi, T., Solar Phys.. 40, 217, 1975.

Palmer, I.D., F.R. Allum, and S. Singer, J. Geophys. Res., 83, 75, 1978.

Parker, E. N., Ap. J., 256, 292, 1982.

Parker, E. N., Ap. J., 128, 664, 1958.

Potter, D. E., Computational Physics, J. Wiley & Sons, Inc., London, 1973.

Pudovkin, M.I., and A.D. Chertkov, Solar Phys, 50, 213, 1976.

Pudovkin, M.I., S.A. Zaitseva, I.P. Oleferenko, and A.D. Chertkov, Solar Phys., 54, 155, 1977.

Pudovkin, M.I., S.A. Zaitseva, and E.E. Benevslenska, J. Geophys. Res., 84, 6649, 1979.

Raadu, M. A., Space Sci. Rev., (in press) 1983.

Richtmeyer, R. D. and Morton, K. W., Difference Methods for Initial Value Problems, (2nd ed), New York/London: Interscience, 1967.

Russell, C.T., and R.L. McPherron, Space Sci. Rev., 28, 121, 1981.

Schüssler, M., Astron. and Astrophys., 56, 439, 1977.

Schüssler, M., Astron. and Astrophys., 71, 79, 1979.

Sen, H. K., and M. L. White, Solar Phys., 23, 146, 1972.

Smith, E.J., Solar wind magnetic field observations, Solar Wind 4, p. 96, ed. by H. Rosenbauer, Max-Planck-Institut für extraterrestrische Physik, Garching W. Germany, 1981.

Spruit, H. C. (1981), Astron. and Astrophys., 98, 155.

Steinolfson, R. S., M. Dryer, and Y. Nakagaura, J. Geophys. Res., 80, 2023, 1975.

Tanaka, K., Solar-Terrestrial Prediction Proceedings, Vol. 3, Cl, ed by R.F. Donnelly, NOAA, Boulder, Colorado, 1979.

Tandberg-Hanssen, E., Solar Activity, Waltham, 1967.

Tang, F., Solar Phys., 75, 179, 1982.

Tang, F., On the Origin of Delta Spots, Big Bear Solar Obs., Cal Tech., April 1982.

Wallenhorst, S. G. and K. P. Topka, Solar Phys., 81, 33, 1982.

Weiss, N. O., Roy. Soc. Lond., A, 293, 310, 1966.

Wu, S. T., S. M. Han, and M. Dryer, Planet. Space Sci., 27, 255, 1979.

Wu, S. T., M. Dryer, and S. M. Han, Solar Phys. (in press), 1963.

Zwickl, R.D., J.R. Asbridge, S.J. Bame, W.C. Feldman, J.T. Gosling, and E.J. Smith, Plasma properties of driver gas following interplanetary shocks observed by ISEE-3, Solar Wind 5, p. 711, ed. by M. Neugebauer, NASA Conf. Pub. 2280, NASA, 1983.